J. Phys. B: At. Mol. Opt. Phys. **31** (1998) 329–339. Printed in the UK PII: S0953-4075(98)87006-5

Momentum-transfer cross section for slow positronium–He scattering

Y Nagashima†, T Hyodo†, K Fujiwara†§ and A Ichimura‡

† Institute of Physics, Graduate School of Arts and Sciences, University of Tokyo, 3-8-1 Komaba, Meguro-ku, Tokyo 153, Japan

‡ Institute of Space and Astronautical Science, 3-1-1 Yoshinodai, Sagamihara, Kanagawa 229, Japan

Received 21 August 1997, in final form 28 October 1997

Abstract. The momentum-transfer cross section for positronium–He scattering has been determined by analysing the thermalization process of orthopositronium in the gas. The momentum distribution of the positronium is observed by using the one-dimensional angular correlation of the annihilation radiation method. Silica aerogel is used to form a sufficient amount of positronium in a restricted region necessary for the high-resolution measurements. The average energies of orthopositronium for mean lifetimes ranging from 3.2 to 86 ns are determined by applying static magnetic fields. A thermalization model which includes the momentum-transfer cross section as an adjustable parameter is fitted to the average energy. The cross section thus obtained is $\sigma_m = (11 \pm 3) \times 10^{-16}$ cm^2 for positronium in the energy range below 0.3 eV.

1. Introduction

The angular correlation of annihilation radiation (ACAR) method provides rich information about the interactions of positronium (Ps) with gas molecules at energies below 1 eV when it is combined with the use of silica aerogel [1]. The silica aerogel permits high angular resolution measurements by producing a large amount of slow Ps in a geometrically small region. The method has been applied to study phenomena such as ortho–para conversion of Ps in O_2 [2, 3], formation of Ps in Xe [4], and thermalization of Ps in various gases [5–7].

In [5, 7], we estimated momentum-transfer cross sections for collisions of Ps with various rare and molecular gases. The average energies for parapositronium (p-Ps) and perturbed orthopositronium which was induced to self-annihilate into two γ-rays by applying a static magnetic field of 0.29 T (we shall refer to the perturbed orthopositronium as o′-Ps) were measured by the ACAR method. The cross sections were estimated from these two values, which correspond to the Ps lifetimes of 0.125 and 50 ns, respectively.

In this work, we have performed improved ACAR measurements on the Ps–He system. The average energies of the o′-Ps for several different lifetimes ranging from 86 to 3.2 ns have been measured by applying static magnetic fields in the range 0.16–1.5 T. These data are analysed in detail to obtain the momentum-transfer cross section. We have derived a differential equation for the Ps thermalization based on the Boltzmann equation, which enables us to take into account the energy-dependent Ps energy loss in collisions with the

§ Deceased.

0953-4075/98/020329+11$19.50

grain surfaces of the silica aerogel. This method provides information on Ps scattering in the energy range below 0.3 eV, which is lower than the range covered by a recently developed variable energy o-Ps beam experiments [8–13].

2. Experimental procedure

The momentum distributions of o-Ps in silica aerogel in 0.92 amagat (1 amagat $\equiv 2.69 \times 10^{25}$ atom m^{-3}, the number density of an ideal gas at 0 °C and 1 atm) of He gas (at a pressure of 1.00 atm) and in vacuum were measured at 296 K using the one-dimensional ACAR apparatus as in previous works [1, 5, 7]. The macroscopic density of the aerogel was 0.1 g cm^{-3}, while the mean grain diameter was 5 nm and the mean distance between the grains was about 70 nm. The momentum resolution of the apparatus was $0.5 \times 10^{-3}mc$ full-width at half-maximum (FWHM), where m and c are the electron mass and speed of light, respectively. The positron source was 3 mCi of ^{22}Na. Magnetic fields up to 1.5 T were applied by using an electromagnet. The 2γ coincidence counts were accumulated with the field pointing parallel ($B > 0$) and antiparallel ($B < 0$) to the average momentum of the positrons impinging on the aerogel. The data for opposite magnetic fields were taken by reversing the field at each angular position of the counter.

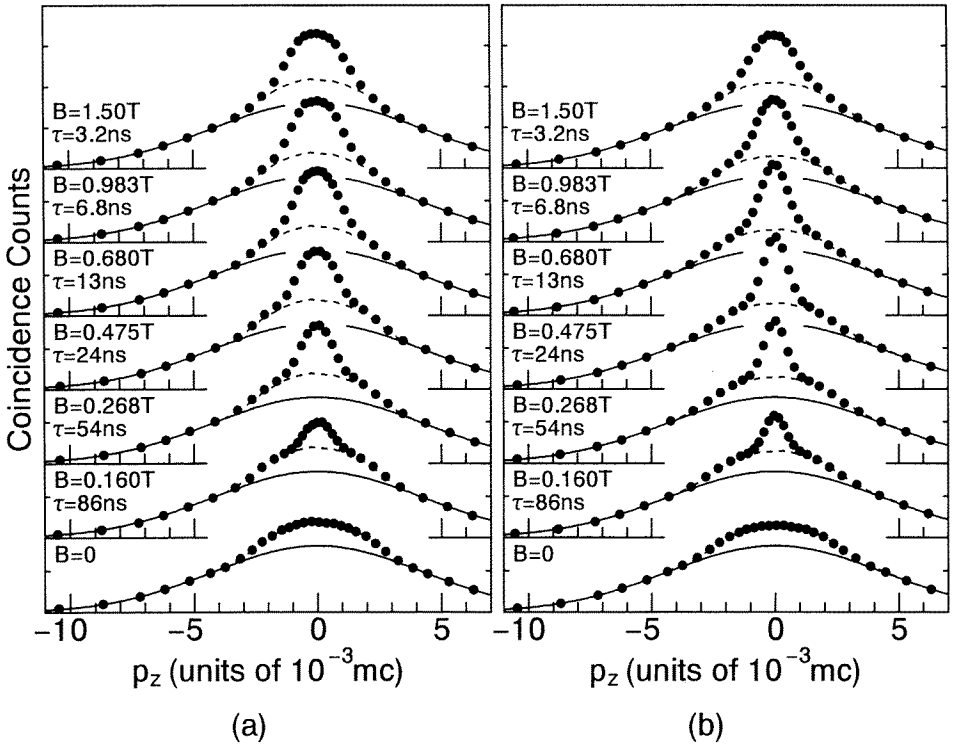

Figure 1. ACAR data for silica aerogel (*a*) in vacuum and (*b*) in 0.92 amagat of He. The full and broken curves show the broad component and the p-Ps component, respectively. All the data are normalized to the same broad component intensity. The values of τ are the calculated mean lifetimes of the o′-Ps.

3. Experimental data and analysis

Figure 1 shows the ACAR data taken in magnetic fields in the range of $B = 0$ to $+1.5$ T. The full curves for the $B = 0$ data are the same Gaussian curves obtained by fitting to the data in the region $|p| \geqslant 5 \times 10^{-3}mc$. They have a FWHM of $10.0 \times 10^{-3}mc$ (broad component). They represent the momentum distribution of the electrons in the silica grains sampled by the positrons [1, 7]. Although the pickoff annihilation of o-Ps also contributes to this component, the fraction is small enough to be neglected. The components above the curves represent the momentum distribution of parapositronium (p-Ps) in the free space between the grains.

In the presence of a magnetic field an additional narrow component appears resulting from the 2γ self-annihilation of the o-Ps perturbed by the magnetic field (o′-Ps). Para-Ps is also perturbed by the field (we shall refer to this Ps as p′-Ps). The annihilation rates of the o′-Ps and p′-Ps are [14]

$$\gamma_{\mathrm{o}'} = \frac{\gamma_{\mathrm{o}} + y^2\gamma_{\mathrm{p}}}{1 + y^2} + \gamma_{\mathrm{pickoff}} \tag{1}$$

and

$$\gamma_{\mathrm{p}'} = \frac{y^2\gamma_{\mathrm{o}} + \gamma_{\mathrm{p}}}{1 + y^2} + \gamma_{\mathrm{pickoff}}, \tag{2}$$

respectively, where γ_{o} and γ_{p} are the self-annihilation rates of the unperturbed o-Ps and p-Ps, and y is given by $y = x/[(1 + x^2)^{1/2} + 1]$ with $x = 4|\mu|B/\bar{h}\omega_0$; μ is the magnetic moment of the electron and $\bar{h}\omega_0$ is the hyperfine structure splitting between o-Ps and p-Ps. For Ps in vacuum, $\gamma_{\mathrm{o}} = 7.04 \times 10^6\ \mathrm{s}^{-1}$, $\gamma_{\mathrm{p}} = 7.99 \times 10^9\ \mathrm{s}^{-1}$, $\mu = -5.79 \times 10^{-5}\ \mathrm{eV\ T}^{-1}$, and $\bar{h}\omega_0 = 8.41 \times 10^{-4}$ eV. The last term, $\gamma_{\mathrm{pickoff}}$, is the Ps pickoff annihilation rate. The value for $\gamma_{\mathrm{pickoff}}$ was determined by measuring the positron lifetime spectrum for the aerogel cut from the same block as that for the ACAR measurement. The obtained values are $6 \times 10^5\ \mathrm{s}^{-1}$ for the aerogel in vacuum and $7 \times 10^5\ \mathrm{s}^{-1}$ for that in 0.92 amagat of He. (These values, which were to be used for the analysis of the ACAR data, were determined by fitting the spectra in the time range including the annihilation of epithermal o-Ps.) The values of τ indicated in figure 1 are the mean lifetimes of the o′-Ps calculated using (1). These values vary widely in the range 86–3.2 ns as B varies from 0.16 to 1.5 T. On the other hand, the mean lifetime of the p′-Ps in the fields of the present experiment remains almost constant; it is 0.130 ns even for $B = 1.5$ T.

If the intensities of the broad component and the p′-Ps component were independent of B, the o′-Ps component could be isolated by subtracting the ACAR data for $B = 0$ from that for $B \neq 0$. Precisely, however, the 2γ self-annihilation intensity of the p′-Ps component depends weakly on the magnitude and the direction of the field due to the spin polarization of the positrons from the β decay [15]. The theoretical intensity is shown in figure 1 of [15], where the intensity of the p′-Ps component varies almost linearly with B. Hence, the average of the intensities for B and $-B$ is almost independent of $|B|$. The lifetime of o′-Ps does not depend on the polarity of B. Thus, the accurate shapes of the o′-Ps component for the field intensity $|B|$ can be obtained by subtracting the ACAR data for $B = 0$ from the average of those for B and $-B$. In the subtraction, the $B = 0$ data as well as the average were normalized to have the same intensity in the momentum region $|p_z| \geqslant 5 \times 10^{-3}mc$. (The pickoff annihilation included in the broad component was neglected in this procedure because the effect was smaller than the statistical error.) The o′-Ps component $N(p_z)$ obtained in this way is shown in figure 2. The p-Ps component is

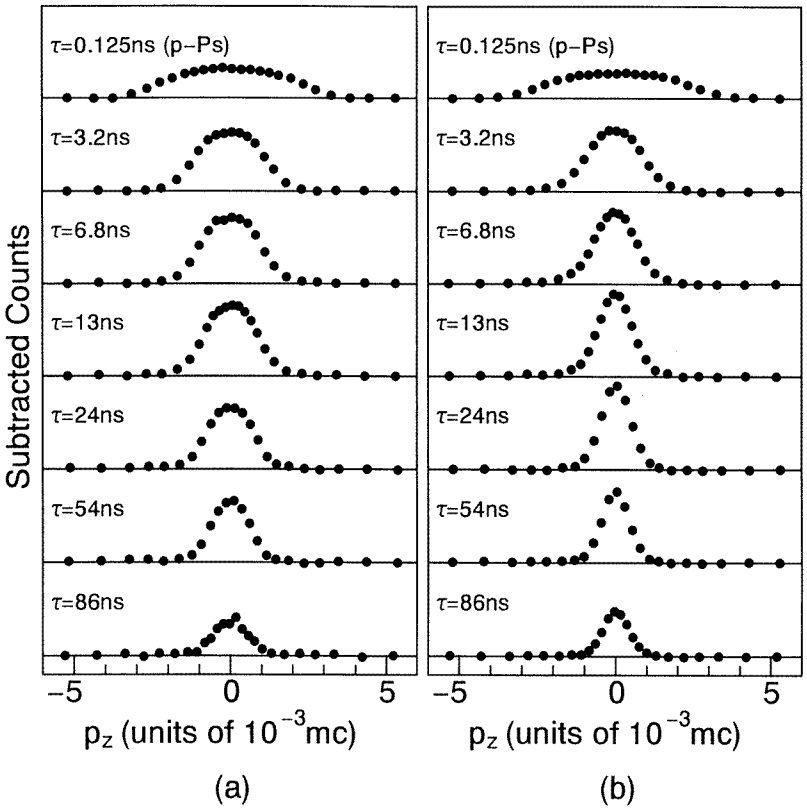

Figure 2. The momentum distributions of p-Ps (top) and those for o′-Ps in (*a*) vacuum and (*b*) 0.92 amagat of He.

shown at the top of this figure. It is clearly seen that the Ps momentum distribution depends on the Ps mean lifetime indicated in the figure.

The average Ps energy $\varepsilon_{\rm av}^{\rm exp}$ can be calculated from $N(p_z)$ as

$$\varepsilon_{\rm av}^{\rm exp} = 3\int_{-\infty}^{\infty} \frac{p_z^2}{2m_{\rm Ps}} N(p_z)\,{\rm d}p_z \Big/ \int_{-\infty}^{\infty} N(p_z)\,{\rm d}p_z \tag{3}$$

where $m_{\rm Ps}$ is the Ps mass. The values of $\varepsilon_{\rm av}^{\rm exp}$ obtained by using (3) for o′-Ps are plotted against τ in figure 3. The effect of the experimental resolution has been corrected by quadratic deconvolution. The open circles in figure 3 are data in vacuum showing the thermalization process of Ps by collisions with the grain surfaces of the silica aerogel, while the full circles show the process in the presence of He atoms in addition.

In the appendix we develop a differential equation describing the thermalization of Ps based on the Boltzmann equation. It gives the foundation for a simpler equation used in previous works [7, 16, 17]. The new equation (A14) incorporates energy-dependent momentum-transfer cross sections.

In a previous analysis of the same data [6], it was noticed that the fractional Ps energy loss per collision with the grain surface decreases with the Ps energy. (This effect has also been noticed in other works [7, 18–20].) It may be explained by the decrease of the phase space available for the phonons created inside and on the surface of the silica grain. In this work we approximate the initial step of the phonon creation by an elastic collision of the Ps

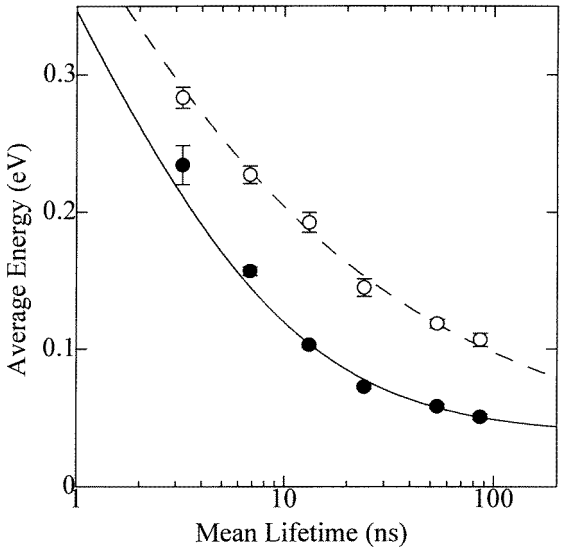

Figure 3. Experimental average energies ($\varepsilon_{\rm av}^{\rm exp}$ see equation (3)) of the o′-Ps in vacuum (open circles) and in 0.92 amagat of He (full circles) plotted against the mean lifetime τ. The broken and full curves are theoretical curves $\varepsilon_{\rm av}^{\rm th}(\tau)$ fitted simultaneously.

with a group of surface atoms [19]. This picture is allowed because the Ps speed is large compared with the speed of the sound in silica [21]. Instead of introducing the effective mass of the surface atoms and the mean-free distance between the grain surfaces as in [19], we simply replace $\frac{2\sigma_m^{(j)}n}{M}$ in (A14) with a parameter s_j. The sum

$$s(E) = \sum_{j=0}^{\infty} s_j \left(\frac{E}{k_B T}\right)^{j/2} \tag{4}$$

then represents the total effect of the grain surfaces which could depend on the Ps energy.

The thermalization process by collisions with He atoms as well as with the grain surface is described by the following equation:

$$\frac{{\rm d}E_{\rm av}(t)}{{\rm d}t} = -\sqrt{2m_{\rm Ps}E_{\rm av}(t)}\left(E_{\rm av}(t) - \frac{3}{2}k_B T\right)\sum_{j=0}^{\infty}\eta_j\left(\frac{2\sigma_m^{(j)}n}{M} + s_j\right)\left(\frac{E_{\rm av}(t)}{k_B T}\right)^{j/2}, \tag{5}$$

where $E_{\rm av}(t)$ is the average Ps energy at time t, n is the number density of He, M is the mass of the He atom, T is the gas temperature, and k_B is the Boltzmann constant. The momentum-transfer cross section has been expanded as equation (A13) and the coefficients η_j are given by equation (A15).

The average energy $\varepsilon_{\rm av}^{\rm exp}$ plotted in figure 3 represents that for Ps with the mean lifetime τ averaged over the time duration for the ACAR measurement, i.e. practically from $t = 0$ to ∞. We should therefore compare $\varepsilon_{\rm av}^{\rm exp}$ with

$$\varepsilon_{\rm av}^{\rm th}(\tau) = \frac{\int_0^{\infty} E_{\rm av}(t){\rm e}^{-t/\tau}\,{\rm d}t}{\int_0^{\infty}{\rm e}^{-t/\tau}\,{\rm d}t}. \tag{6}$$

We first analysed the energy dependence of s. We determined the average value of $s(E)$ for two adjacent points for vacuum shown in figure 3 by assuming that $s(E)$ is constant

in the regions between adjacent two points. Equation (5) takes the following form when $\bar{s} = s_0$ ($s_j = 0$ for $j \neq 0$) and $n = 0$:

$$\frac{\mathrm{d}}{\mathrm{d}t}E_{\mathrm{av}}(t) = -\sqrt{2m_{\mathrm{Ps}}E_{\mathrm{av}}(t)}\left(E_{\mathrm{av}}(t) - \frac{3}{2}k_BT\right)\frac{8}{3}\sqrt{\frac{2}{3\pi}}\bar{s}. \tag{7}$$

The solution of this equation is

$$E_{\mathrm{av}}(t) = \left(\frac{1 + A\mathrm{e}^{-bt}}{1 - A\mathrm{e}^{-bt}}\right)^2 \frac{3}{2}k_BT, \tag{8}$$

where

$$b = \frac{8}{3}\sqrt{\frac{2}{3\pi}}\bar{s}\sqrt{3m_{\mathrm{Ps}}k_BT}, \tag{9}$$

and A is a constant determined by the initial average energy of Ps. When $E_{\mathrm{av}}(t)$ is given by (8), $\varepsilon_{\mathrm{av}}^{\mathrm{th}}(\tau)$ can be expanded as

$$\varepsilon_{\mathrm{av}}^{\mathrm{th}}(\tau) = \left(1 + \sum_{k=1}^{\infty}\frac{4kA^k}{1 + b\tau k}\right)\frac{3k_BT}{2}. \tag{10}$$

The values of $\bar{s}$ in equation (9) determined by solving the simultaneous equation of type (10) for the two adjacent points were plotted in figure 4 against the average energy of the two points. This figure shows that the effect of the collision with the grain surfaces certainly decreases with the Ps energy. For the sake of simplicity, we assume that energy dependence of s can be represented by a power law

$$s(E) \propto \left(\frac{E_{\mathrm{av}}}{k_BT}\right)^{\beta} \tag{11}$$

over the limited range of this experiment, where β is a constant. (The full line in figure 4 represents $\beta = 2.2$ as determined below.)

It is difficult to analyse the data if we take into account the energy dependencies of both $s(E)$ and $\sigma_m(E)$. Therefore, we assume that the momentum-transfer cross section for He is constant over the energy range of interest. The differential equation for $E_{\mathrm{av}}(t)$ is then simplified as follows

$$\frac{\mathrm{d}}{\mathrm{d}t}E_{\mathrm{av}}(t) = -\sqrt{2m_{\mathrm{Ps}}E_{\mathrm{av}}(t)}\left(E_{\mathrm{av}}(t) - \frac{3}{2}k_BT\right)\left(\frac{8}{3}\sqrt{\frac{2}{3\pi}}\frac{2\sigma_m n}{M} + \alpha\left(\frac{E_{\mathrm{av}}(t)}{k_BT}\right)^{\beta}\right), \tag{12}$$

where α is a constant. (We assume here that (5), which is given only for j being integer, is valid for any real value.) The theoretical Ps average energy $\varepsilon_{\mathrm{av}}^{\mathrm{th}}(\tau)$ is determined from equations (6) and (12) numerically for given $E_{\mathrm{av}}(0)$, σ_m, α and β. We performed nonlinear least-squares fit of $\varepsilon_{\mathrm{av}}^{\mathrm{th}}(\tau)$ to $\varepsilon_{\mathrm{av}}^{\mathrm{exp}}$ for both the data in vacuum and in He simultaneously. The value of $E_{\mathrm{av}}(0)$ was fixed to be 0.8 eV, which is the Ps emission energy from silica grains [7]. The outcome of the fit is insensitive to this value. We also tried fixing $E_{\mathrm{av}}(0)$ to be the value in the range between 0.8 and 6.8 eV, which includes the Ps emission energy from quartz single crystal measured by Sferlazzo *et al* [22]. The results are almost the same as that for 0.8 eV. The optimized parameters are

$$\sigma_m = 11 \times 10^{-16}\ \mathrm{cm}^2, \tag{13}$$

$$\beta = 2.2, \tag{14}$$

and

$$\alpha = 3.0 \times 10^{30}\ \mathrm{kg}^{-1}\ \mathrm{m}^{-1}. \tag{15}$$

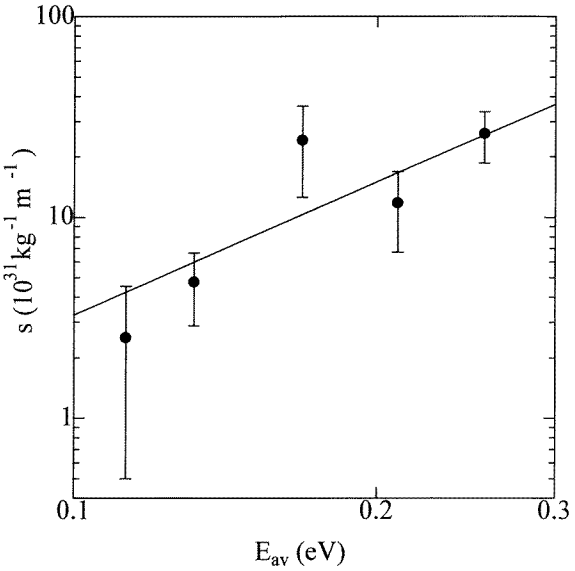

Figure 4. The values of the parameter s plotted against average o′-Ps energy. The full line shows power law dependence $\alpha(E_{\rm av}/k_BT)^{2.2}$.

The simultaneously fitted curves are shown in figure 3. The full line shown in figure 4 is the fitted function of the form (11) with β being fixed to be 2.2.

We also performed the fitting with β being constrained to an integer or a half-integer. If we assume that $\beta = 2$ or $\frac{5}{2}$, the fit is almost as good as that for $\beta = 2.2$. The optimized value of σ_m is also the same as equation (13).

By considering the statistical and systematic errors in the estimation of $\varepsilon_{\rm av}^{\rm exp}$, we determined the momentum-transfer cross section in the Ps energy range below 0.3 eV as follows

$$\sigma_m = (11 \pm 3) \times 10^{-16}\ {\rm cm}^2 = (13 \pm 4)\pi a_0^2, \tag{16}$$

where a_0 is the Bohr radius.

The momentum-transfer cross section for this system was also estimated from the ACAR data for lower gas density [23] in order to check the systematic effect. The density was 0.184 amagat, and a magnetic field of 0.29 T was applied. The momentum-transfer cross section obtained with β being fixed to be 2.2 is $\sigma_m = 9 \times 10^{-16}$ cm^2, which agrees with the value given in equation (16) within the error.

4. Discussion

The value of σ_m is improved on that estimated in the previous work [7] where the Ps average energies only for the mean lifetimes of 0.125 and 50 ns were measured. The previous value is a few times larger than the present value. This is because the energy dependence of the Ps energy loss on collision with the grain surfaces was not taken into account. The present value is also improved on the value in [6] where the average energy for the Ps mean lifetime τ was compared with a value obtained from the simple model at time τ without the averaging procedure (6).

The ‘collision cross section’ of Ps in He was estimated by Spektor and Paul [24]

experimentally from a Ps lifetime measurement long ago. Their value is three orders of magnitude smaller than the present value. Garner *et al* [12] measured the Ps total scattering cross section in He using the Ps beam. The value is 2.8–5.1 $\times 10^{-16}$ cm^2 in the 10–110 eV Ps energy range; no data in the present energy range are reported. The discrepancy between these values and our result might indicate that there is a strong energy dependence of the cross section. Coleman *et al* [25] estimated the Ps scattering cross section in He, Ne, and Ar from two-dimensional ACAR measurements. They used the gas itself as Ps formation medium. Although they only gave a common value of $(9 - 0.5E)\pi\ a_0^2$ for all the gases where E is the Ps energy in eV, it is of the same order of magnitude as the present result for He.

Theoretical investigations on the Ps–He system have also been performed by several authors [26–30]. The momentum-transfer cross section at 0.272 eV evaluated in [26, 27] are 10.6×10^{-16} cm^2 and 8.25×10^{-16} cm^2, respectively. These values agree with the present result within the error. The total scattering cross section for $E = 0$ was also calculated by Drachman and Houston [28] and Peach [29]. The obtained values are 6.8×10^{-16} cm^2 and 3.3×10^{-16} cm^2, respectively. Both values are smaller than our value. McAlinden *et al* [30] calculated the total scattering cross section in the Ps energy range below 100 eV but did not report values in the present energy range.

5. Conclusion

We have analysed the thermalization of Ps in 1 atm of He gas observed by the ACAR method with silica aerogel, and obtained the momentum-transfer cross section for Ps–He collisions. The result is $\sigma_m = (11 \pm 3) \times 10^{-16}$ cm^2 $= (13 \pm 4)\pi a_0^2$ for Ps in the energy range below 0.3 eV.

Acknowledgments

We thank Professor Y Itikawa, Dr M Charlton and Dr P Van Reeth for valuable discussions. We also thank Dr T Chang for providing us with the silica aerogel. This work was partly supported by the Japanese Ministry of Science, Culture and Education grant no 63460037 and by Matsuo Foundation. The experiments were performed at the Radioisotope Center of the University of Tokyo.

Appendix

In this appendix, we derive a differential equation describing the time evolution of the Ps average energy in gas. It is used in section 3, where we determine the momentum-transfer cross section through fitting with the average energies measured for different Ps mean lifetimes.

Under the present experimental condition, the number density, n, of the gas is overwhelmingly higher than the number density of the Ps atoms. Accordingly, we only take into account the elastic scattering by the gas molecules, ignoring the scattering by other Ps. We also assume that the gas remains in thermal equilibrium (velocity distribution $F(\boldsymbol{V})$) during the Ps thermalization process. Thus, the time evolution of the Ps velocity distribution function $f(\boldsymbol{v}, t)$ is governed by the linear Boltzmann equation,

$$\frac{\partial f(\boldsymbol{v}, t)}{\partial t} = \int \mathrm{d}\boldsymbol{v}' \, [w(\boldsymbol{v}' \to \boldsymbol{v}) f(\boldsymbol{v}', t) - w(\boldsymbol{v} \to \boldsymbol{v}') f(\boldsymbol{v}, t)]. \tag{A1}$$

Here $w(\boldsymbol{v} \to \boldsymbol{v}')$ represents the transition probability per unit time due to the scattering, where the velocities of Ps (mass $m_{\rm Ps}$) and the gas molecules (mass M) change as $(\boldsymbol{v}, \boldsymbol{V}) \to (\boldsymbol{v}', \boldsymbol{V}')$. It is written with the cross section σ as

$$w(\boldsymbol{v} \to \boldsymbol{v}') = n \int \mathrm{d}\boldsymbol{V}\, F(\boldsymbol{V}) \int \mathrm{d}\boldsymbol{V}'\, \delta^{(3)}(\boldsymbol{v}_g - \boldsymbol{v}_g') \left[v_r \frac{\mathrm{d}\sigma(\boldsymbol{v}_r \to \boldsymbol{v}_r')}{\mathrm{d}\boldsymbol{v}_r'} \right]. \tag{A2}$$

These transitions are also expressed in terms of the relative and the centre-of-mass velocities as $(\boldsymbol{v}_r, \boldsymbol{v}_g) \to (\boldsymbol{v}_r', \boldsymbol{v}_g')$, where $\boldsymbol{v}_r \equiv \boldsymbol{v} - \boldsymbol{V}$ and $\boldsymbol{v}_g \equiv (m_{\rm Ps}\boldsymbol{v} + M\boldsymbol{V})/(m_{\rm Ps} + M)$. The notation for the derivative of σ used in (A2) is related to the differential cross section $\frac{\mathrm{d}\sigma}{\mathrm{d}\Omega}$ as,

$$\frac{\mathrm{d}\sigma(\boldsymbol{v} \to \boldsymbol{v}')}{\mathrm{d}\boldsymbol{v}'} = \frac{1}{v^2}\delta(v - v')\frac{\mathrm{d}\sigma}{\mathrm{d}\Omega}. \tag{A3}$$

Noting this relation, the momentum-transfer cross section can be written as

$$\sigma_m(v) = \int \mathrm{d}\boldsymbol{v}'\, \frac{\mathrm{d}\sigma(\boldsymbol{v} \to \boldsymbol{v}')}{\mathrm{d}\boldsymbol{v}'}(1 - \hat{\boldsymbol{v}} \cdot \hat{\boldsymbol{v}}'), \tag{A4}$$

where $\hat{\boldsymbol{v}} = \boldsymbol{v}/|\boldsymbol{v}|$ and $\hat{\boldsymbol{v}}' = \boldsymbol{v}'/|\boldsymbol{v}'|$.

Using the Boltzmann equation (A1), the time derivative of the Ps average energy $E_{\rm av}(t)$ is expressed as

$$\frac{E_{\rm av}(t)}{\mathrm{d}t} = -\frac{m_{\rm Ps}M}{m_{\rm Ps} + M} \int \mathrm{d}\boldsymbol{v} \int \mathrm{d}\boldsymbol{v}'\, w(\boldsymbol{v} \to \boldsymbol{v}') f(\boldsymbol{v}, t) \boldsymbol{v}_g \cdot (\boldsymbol{v}_r - \boldsymbol{v}_r'). \tag{A5}$$

This equation can be rewritten as

$$\frac{\mathrm{d}E_{\rm av}(t)}{\mathrm{d}t} = -\int \mathrm{d}\boldsymbol{v}\, f(\boldsymbol{v}, t) W(v);\ W(v) \equiv n\frac{m_{\rm Ps}M}{m_{\rm Ps} + M} \int \mathrm{d}\boldsymbol{V}\, F(\boldsymbol{V}) \boldsymbol{v}_g \cdot \boldsymbol{v}_r [v_r \sigma_m(v_r)]. \tag{A6}$$

Here we have used (A2) and applied the formula derived from (A4):

$$\int \mathrm{d}\boldsymbol{v}'\, \frac{\mathrm{d}\sigma(\boldsymbol{v} \to \boldsymbol{v}')}{\mathrm{d}\boldsymbol{v}'} \boldsymbol{a} \cdot (\boldsymbol{v} - \boldsymbol{v}') = \boldsymbol{a} \cdot \boldsymbol{v}\sigma_m(v), \tag{A7}$$

which is valid for any constant vector $\boldsymbol{a}$.

Noting that M is much larger than $m_{\rm Ps}$ (by a factor of about 10^4), we expand the factor $W(v)$ in (A6) in terms of a small parameter $m_{\rm Ps}/M$, so that we obtain

$$W(v) = \left[\frac{E}{k_B T} - \frac{3}{2} - E\frac{\mathrm{d}}{\mathrm{d}E} \right] \omega(E); \qquad \omega(E) \equiv n\frac{2m_{\rm Ps}}{M} k_B T [v\sigma_m(v)], \tag{A8}$$

where k_B denotes the Boltzmann constant, T being the gas temperature. The factor $k_B T$ comes from the thermal distribution $F(\boldsymbol{V})$ of the gas molecules. In the $m_{\rm Ps}/M$ expansion, we have assumed $\mathrm{O}((V/v)^2) = \mathrm{O}(m_{\rm Ps}/M)$ for the velocities. This procedure is justified because the average energy of Ps is near the thermal energy (within a factor of 7 at most) through the present analysis.

To get a closed differential equation for the $E_{\rm av}(t)$, we assume that the $f(\boldsymbol{v}, t)$ on the right-hand side of (A6) has a Maxwellian form at any time, as

$$\int \mathrm{d}\boldsymbol{v}\, f(\boldsymbol{v}, t) \cdot \Longrightarrow \int_0^\infty \mathrm{d}E\, f_M(E; T^*(t)) \cdot, \tag{A9}$$

where the effective temperature $T^*(t)$ is defined as

$$\tfrac{3}{2} k_B T^*(t) \equiv E_{\rm av}(t), \tag{A10}$$

i.e.

$$f_M(E; T^*(t)) \equiv \frac{2}{\sqrt{\pi}} (k_B T^*(t))^{-\frac{3}{2}} \sqrt{E} \exp\left(-\frac{E}{k_B T^*(t)} \right). \tag{A11}$$

This procedure is expected to be a good approximation at least near the thermal equilibrium. By applying the replacement (A9) to (A6) and substituting (A8), the following equation is obtained:

$$\frac{\mathrm{d}}{\mathrm{d}t}\left[\frac{3}{2}k_BT^*(t)\right] = \left(\frac{1}{k_BT^*(t)} - \frac{1}{k_BT}\right)\int_0^\infty \mathrm{d}E\, f_M(E;T^*(t))E\omega(E). \tag{A12}$$

This equation determines the time evolution of $E_{\mathrm{av}}(t)$.

If the energy-dependent momentum-transfer cross section is expanded by a power series

$$\sigma_m(E) = \sum_{j=0}^{\infty}\sigma_m^{(j)}\left(\frac{E}{k_BT}\right)^{j/2}, \tag{A13}$$

(A12) is reduced to the form, after replacing $T^*(t)$ back to $E_{\mathrm{av}}(t)$,

$$\frac{\mathrm{d}E_{\mathrm{av}}(t)}{\mathrm{d}t} = -\sqrt{2m_{\mathrm{Ps}}E_{\mathrm{av}}(t)}\left(E_{\mathrm{av}}(t) - \frac{3}{2}k_BT\right)\sum_{j=0}^{\infty}\eta_j\frac{2\sigma_m^{(j)}n}{M}\left(\frac{E_{\mathrm{av}}(t)}{k_BT}\right)^{j/2}, \tag{A14}$$

where η_j represents

$$\eta_j \equiv \left\{\begin{array}{ll} (j+4)!!(\frac{1}{3})^{\frac{j+3}{2}}; & \text{for} \quad j = \text{odd} \\ \dfrac{2}{\sqrt{\pi}}\left(\dfrac{j+4}{2}\right)!\left(\dfrac{2}{3}\right)^{\frac{j+3}{2}}; & \text{for} \quad j = \text{even} \end{array}\right\}. \tag{A15}$$

References

[1] Hyodo T 1992 *Positron Annihilation (Materials Science Forum 105–110)* ed Zs Kajcsos and Cs Szeles (Aedermannsdorf: Trans Tech) p 281
[2] Kakimoto M, Hyodo T, Chiba T, Akahane T and Chang T B 1987 *J. Phys. B: At. Mol. Phys.* **20** L107
[3] Kakimoto M, Hyodo T and Chang T B 1990 *J. Phys. B: At. Mol. Opt. Phys.* **23** 589
[4] Kakimoto M and Hyodo T 1988 *J. Phys. B: At. Mol. Opt. Phys.* **21** 2977
[5] Kakimoto M, Nagashima Y, Hyodo T, Fujiwara K and Chang T B 1989 *Positron Annihilation* ed L Dorikens-Vanpraet, M Dorikens and D Segers (Singapore: World Scientific) p 737
[6] Nagashima Y, Hyodo T and Fujiwara K 1992 *Positron Annihilation (Materials Science Forum 105–110)* ed Zs Kajcsos and Cs Szeles (Aedermannsdorf: Trans Tech) p 1671
[7] Nagashima Y *et al* 1995 *Phys. Rev.* A **52** 258
[8] Zafar N, Laricchia G, Charlton M and Griffith T C 1991 *J. Phys. B: At. Mol. Opt. Phys.* **24** 4661
[9] Zafar N, Laricchia G and Charlton M 1994 *Hyperfine Interact.* **89** 243
[10] Laricchia G 1995 *Nucl. Instrum. Methods* B **99** 363
[11] Zafar N, Laricchia G, Charlton M and Garner A 1996 *Phys. Rev. Lett.* **76** 1595
[12] Garner A J, Laricchia G and Özen A 1996 *J. Phys. B: At. Mol. Opt. Phys.* **29** 5961
[13] Laricchia G 1996 *Hyperfine Interact.* **100** 71
[14] Halpern O 1954 *Phys. Rev.* **94** 904
[15] Nagashima Y and Hyodo T 1990 *Phys. Rev.* B **41** 3937
[16] Sauder W C 1968 *J. Res. NBS* A **72** 91
[17] Dauwe C, Consolati G, Van Hoecke T and Segers D 1996 *Nucl. Instrum. Methods* A **371** 497
[18] Chang T, Xu M and Zeng X 1987 *Phys. Lett.* **126A** 189
[19] Hyodo T, Kakimoto M, Chang T B, Deng J, Akahane T, Chiba T, McKee B T A and Stewart A T 1989 *Positron Annihilation* ed L Dorikens-Vanpraet, M Dorikens and D Segers (Singapore: World Scientific) p 878
[20] Mills A P Jr, Shaw E D, Chichester R J and Zuckerman D M 1989 *Phys. Rev.* B **40** 2045
[21] Ford G W, Sander L M and Witten T A 1976 *Phys. Rev. Lett.* **36** 1269
[22] Sferlazzo P, Berko S and Canter K F 1987 *Phys. Rev.* B **35** 5315
[23] Kakimoto M 1987 *PHD Thesis* (in Japanese)
[24] Spektor D M and Paul D A L 1975 *Can. J. Phys.* **53** 13
[25] Coleman P G, Rayner S, Jacobsen F M, Charlton M and West R N 1994 *J. Phys. B: At. Mol. Opt. Phys.* **27** 981

[26] Fraser P A 1961 *Proc. Phys. Soc.* **79** 721
Fraser P A and Kraidy M 1966 *Proc. Phys. Soc.* **89** 533
Fraser P A 1968 *J. Phys. B: At. Mol. Phys.* **1** 1006
[27] Barker M I and Bransden B H 1968 *J. Phys. B: At. Mol. Phys.* **1** 1109
Barker M I and Bransden B H 1969 *J. Phys. B: At. Mol. Phys.* **2** 730
[28] Drachman R J and Houston S K 1970 *J. Phys. B: At. Mol. Phys.* **3** 1657
[29] Peach G 1995 *Positron Spectroscopy of Solids* ed A Dupasquier and A P Mills Jr (Amsterdam: IOS) p 401
(cited by G Laricchia)
[30] McAlinden M T, MacDonald F G R S and Walters H R J 1996 *Can. J. Phys.* **74** 434